Organic LETTERS

Letter

pubs.acs.org/OrgLett

Hydrogen-Bond Controlled π-Dimerization in Viologen-Appended Calixarenes: Revealing a Subtle Balance of Weak Interactions

Christophe Kahlfuss,[†] Anne Milet,[‡] Jennifer Wytko,[§] Jean Weiss,[§] Eric Saint-Aman,*[,‡] and Christophe Bucher*[,†]

[†]Laboratoire de Chimie (UMR 5182), École Normale Supérieure de Lyon/CNRS Université de Lyon 1, Lyon, France

[‡]Département de Chimie Moléculaire (UMR 5250), Université Joseph Fourier/CNRS, Grenoble, France

[§]Institut de Chimie, UMR 7177 CNRS-Université de Strasbourg, 1 rue Blaise Pascal, 67008 Strasbourg cedex, France

Supporting Information

ABSTRACT: The intramolecular π-dimerization between two 4,4′-bipyridinium cation radicals directly connected to the wide rim of a calixarene is described. The ability of a phenol-containing calixarene to dimerize in its two-electron-reduced state depends on a subtle balance of weak interactions associated with hydrogen bond formation on the lower rim and orbital overlap between π-radicals on the upper rim.

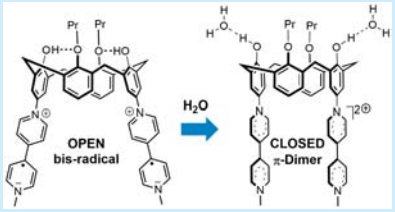

Viologen cation-radicals are known to undergo noncovalent π-dimerization processes yielding "long-bonded" cofacial supramolecular complexes.[1] The reversible formation of the "π-bond" holding both radicals at sub-van der Waals distances in sandwich-like structures arises from the orbital overlaps occurring between the SOMOs centered on both π-systems. The resulting π-dimers display characteristic signatures which can be readily identified by vis/NIR and ESR spectroscopy measurements or by cyclic voltammetry. The unique structure and properties of these noncovalent dimeric assemblies of viologens associated and dissociated under redox control have proven to be particularly useful for the design of both redox-responsive molecular machines and materials.[2] The most straightforward strategy employed so far to enhance the dimerization has been to connect the viologen cation radicals via covalent linkers of appropriate sizes and flexibilities.[1a] This approach has led to the development of numerous rigid systems that hold two radicals in a cofacial arrangement and has also generated more flexible architectures in which significant molecular motions are associated with dimerization.

Following our results on redox-responsive molecular systems,[3] we now wish to report a detailed analysis of the π-dimerization occurring between two bipyridinium radical cations directly connected to a calixarene hinge. We show that the calixarene linker is flexible enough to allow the formation of an intramolecular π-dimer between both π-radicals introduced at the upper rim.[4] Most importantly, the overall conformation of the molecule has been established and its ability to form a π-dimer is governed by a subtle energetic balance between two types of "weak" interactions localized on each rim of the calixarene platform. The π-dimerization only occurs at the wider upper rim when the associated stabilization energy becomes large enough to counterbalance the energy of the H-bond network involving the phenol units at the narrow lower rim.

The two calixarene-bipyridinium targets 4^{4+} and 7^{4+} were prepared following the synthetic route in Scheme 1. Both

Scheme 1

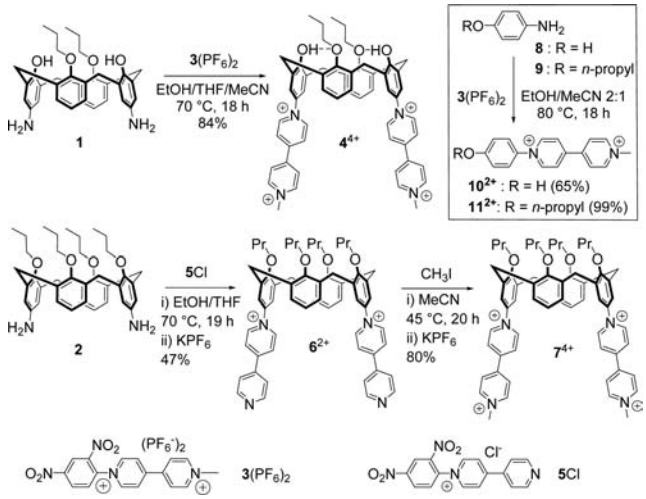

compounds bear two 4,4′-bipyridiniums directly connected to the calixarene's wide rim. The two scaffolds differ in their substitution pattern of the four lower rim OH functions. Four propoxyl substituents were introduced at the lower rim of compound 7^{4+} whereas only two of the four hydroxyl substituents were substituted in 4^{4+}. The starting calix[4]arenes **1** and **2** were synthesized according to reported procedures involving the O-alkylation of the calix[4]arene followed by nitration with nitric acid and reduction with $SnCl_2$.[5] A variant of

Received: July 10, 2015
Published: August 13, 2015

DOI: 10.1021/acs.orglett.5b01982
Org. Lett. 2015, 17, 4058–4061

the Zincke reaction allowed the introduction of bipyridinium moieties at the upper rim of the calixarene skeleton. Compounds $\mathbf{3}^{2+}$ and $\mathbf{5}^{+}$ were synthesized from 2,4-dinitro-chlorobenzene and 4,4′-bipyridine or 1-methyl-4,4′-bipyridinium, respectively.[6] The primary amine available at the wider rim of the calixarene precursor **1** or **2** reacted at high temperature with an excess of the dinitrophenyl-pyridinium derivative $\mathbf{3}^{2+}$ or $\mathbf{5}^{+}$ to afford the bis-viologen calix[4]arene $\mathbf{4}^{4+}$ and the pyridine-pyridinium-substituted calix[4]arene $\mathbf{6}^{2+}$, respectively. The latter was eventually quaternized with CH_3I to yield $\mathbf{7}^{4+}$, followed by anion exchange with KPF_6. We have observed that dimerization was unaffected by the nature of the counterion. Similar Zincke-type procedures were used to synthesize the reference compounds $\mathbf{10}^{2+}$ and $\mathbf{11}^{2+}$. Although compound $\mathbf{7}^{4+}$ could potentially be obtained in one step by reacting **2** with $\mathbf{3}^{2+}$, the two-step strategy used was justified by our interest in intermediate $\mathbf{6}^{2+}$ for another project.

The ^{1}H NMR characterization of $\mathbf{4}^{4+}$ and $\mathbf{7}^{4+}$ in CD_3CN (Figure ESI 9) supports the cone conformation of the calixarene. The existence of H-bonds involving the pendant phenolic groups at the lower rim in $\mathbf{4}^{4+}$ (Scheme 1) was initially revealed by the deshielded resonance of the hydroxyl protons at 9.48 ppm in the spectrum of $\mathbf{4}^{4+}$ when compared to the reference compound $\mathbf{10}^{2+}$ (7.86 ppm). These H-bonds were preserved in the presence of a strong H-bond acceptor such as DMSO, as shown by the similarity of the spectra in CD_3CN and DMSO-d_6 (Figure ESI 10). The rigidity of the calixarene scaffold induced by the H-bond network at the lower rim is also evidenced by comparing the chemical shifts of $\mathbf{4}^{4+}$ with those of the "flexible" H-bond free analog $\mathbf{7}^{4+}$; the protons of the calixarene's aromatic rings bearing no viologens are shielded in the spectrum of $\mathbf{7}^{4+}$ compared to that of $\mathbf{4}^{4+}$ (Figure ESI 9). This shielding is attributed to a more parallel arrangement of these aromatic rings in $\mathbf{7}^{4+}$ compared to their position in $\mathbf{4}^{4+}$ where H-bonding creates an open cone conformation.[7] The pairs of doublets for the $ArCH_2Ar$ protons are also affected by the more or less open cone conformation.[7b]

The ability of bipyridinium cation-radicals derived from $\mathbf{4}^{4+}$ and $\mathbf{7}^{4+}$ to form π-dimers in solution was studied by electrochemistry. The voltammetric curves recorded for $\mathbf{4}^{4+}$ and $\mathbf{7}^{4+}$ in electrolytic DMF solutions (Figure 1) exhibit the

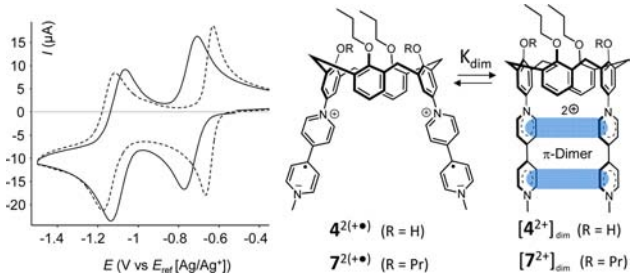

Figure 1. CV curves of $\mathbf{4}(PF_6)_4$ (solid line) and $\mathbf{7}(PF_6)_4$ (dotted line), 1 mM in DMF (TBAP 0.1 M, v = 0.1 V/s).

expected two consecutive bipyridinium-centered cathodic waves at −0.5 and −1.5 V. Each wave accounts for two electrons per molecule (one e^-/bipyridinium fragment) yielding successively the diradical $\mathbf{X}^{2(+\bullet)}$ and the neutral species $\mathbf{X}^0$ (with X = **4** or **7**).

The electrochemical response of both compounds remains diffusion-controlled up to v = 3 V s^{-1} as judged from the linear increase of the peak intensity versus $v^{1/2}$ and from the stability of the peak-to-peak separation, ΔE_p, over this time-scale range (Figure ESI 1). The electrochemical data corresponding to these two consecutive reduction waves are collected in Table ESI 1 along with those of $\mathbf{10}^{2+}$ and $\mathbf{11}^{2+}$ used as reference compounds. The first bipyridinium-centered reduction in $\mathbf{4}^{4+}$ occurs at a potential close to the reference values observed for $\mathbf{10}^{2+}$ or $\mathbf{11}^{2+}$, i.e. at $E_{1/2} \approx -0.74$ V, with a ΔE_p of ca. 60 mV at 0.1 V s^{-1}. Further reduction leading to the neutral, fully reduced species is achieved around −1.1 V for both $\mathbf{4}^{4+}$ and $\mathbf{10}^{2+}$. These data thus support a similar behavior for both species, with no π-dimers forming from $\mathbf{4}^{2(+\bullet)}$ or $\mathbf{10}^{+\bullet}$ under our experimental conditions. This behavior differs from that of $\mathbf{7}^{4+}$ for which the first cathodic wave is shifted toward a more positive potential by more than 100 mV, i.e. at $E_{1/2} \approx -0.65$ V, with a ΔE_p = 37 mV at 0.1 V s^{-1} (Figure 1 and Table ESI 1). The latter value is much lower than the value of 60 mV expected for one-electron Nernstian transfers or for multielectron Nernstian transfers centered on molecules bearing multiple, fully independent and chemically equivalent, redox centers.

In addition, the stability domain of the first, two-electron reduced form, $\mathbf{7}^{2(+\bullet)}$, is extended by *ca.* 0.14 V compared to that of $\mathbf{4}^{2(+\bullet)}$ (Figure 1). These findings support a stabilization of the electrogenerated di(cation radical) $\mathbf{7}^{2(+\bullet)}$ upon formation of the intramolecular π-dimer $[\mathbf{7}^{2+}]_{dim}$, in which the orbital overlap occurs between two π-radicals at sub-van der Waals distances in a cofacial conformation (Figure 1). These interactions involving unpaired π-electrons are only observed with the *per* O-alkylated compound $\mathbf{7}^{4+}$ and not with the partially substituted analogue $\mathbf{4}^{4+}$. The non-O-substituted phenol units at the lower rim of the calixarene hamper the coupling between both radicals located on the opposite rim (Figure 1).

The potentials of the first and second reduction processes remain unchanged over the 0.05 to 1 mM concentration range, demonstrating the intramolecular character of the π-dimerization $\mathbf{7}^{2(+\bullet)} \leftrightarrow [\mathbf{7}^{2+}]_{dim}$. This conclusion is also supported by spectroelectrochemistry experiments carried out on $\mathbf{4}^{2+}$, $\mathbf{7}^{4+}$, $\mathbf{10}^{4+}$ and $\mathbf{11}^{2+}$ (Figure 2). The UV/vis spectra recorded during exhaustive

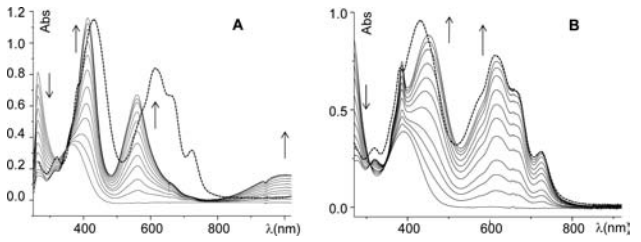

Figure 2. UV/vis spectra recorded during the exhaustive reduction (1 e−/$\mathbf{BP}^{2+}$) of (A) $\mathbf{7}^{4+}$ and (B) $\mathbf{4}^{4+}$ in DMF (0.1 M TBAP); E = −0.9 V (0.25 mM, 15 mL, time ≈ 30 min). Dashed lines: UV/vis spectra of (A) $\mathbf{11}^{+\bullet}$ and (B) $\mathbf{10}^{+\bullet}$, 0.5 mM in DMF (0.1 M TBAP). Path length: 1 mm.

electrolyses of $\mathbf{4}^{4+}$ and $\mathbf{10}^{2+}$ in DMF confirm the accumulation of nonassociated viologen radicals that are easily identified from the bands growing at 615 nm (29900 L mol^{-1} cm^{-1}), 450 nm (35300 L mol^{-1} cm^{-1}) and 386 nm (29900 L mol^{-1} cm^{-1}). In both cases, the ESR spectrum of the fully electrolyzed solution (1e^-/$\mathbf{BP}^{2+}$) displays an intense signal centered at g= 2.00045 and attributed to noninteracting bipyridinium cation radicals in $\mathbf{4}^{2(+\bullet)}$ or $\mathbf{10}^{+\bullet}$ (Figure ESI 3). The UV/vis and ESR data recorded over the course of a two-electron electrolysis of a DMF electrolytic solution of the per O-alkylated compound $\mathbf{7}^{4+}$ (Figure 2A) conversely support the formation of the π-dimerized species $[\mathbf{7}^{2+}]_{dim}$. The most convincing experimental evidence is the progressive growth of the diagnostic absorption bands at 413 nm (46300 L mol^{-1} cm^{-1}), 560 nm (26800 L mol^{-1} cm^{-1}) and *ca.*

DOI: 10.1021/acs.orglett.5b01982
Org. Lett. 2015, 17, 4058−4061

1000 nm (6500 L mol^{-1} cm^{-1}), as well as the ESR silent signature of the fully electrolyzed solution (Figure ESI 3). The intramolecular character of the dimerization was further established by spectro-electrochemistry experiments carried out in the same viologen concentration range with the reference compounds $\mathbf{10}^{2+}$ and $\mathbf{11}^{2+}$. These experiments showed that the one-electron electrochemical reduction exclusively yielded the cation radicals $\mathbf{10}^{+\bullet}$ and $\mathbf{11}^{+\bullet}$, respectively.

Two different behaviors were thus observed with $\mathbf{4}^{4+}$ and $\mathbf{7}^{4+}$. All experimental data support the conclusion that the two-electron reduction of $\mathbf{7}^{4+}$, featuring four noninteracting propoxyl units at the calixarene's lower rim, yields the diamagnetic intramolecular π-dimer $[\mathbf{7}^{2+}]_{dim}$ whereas, under the same conditions, $\mathbf{4}^{4+}$ yields the noninteracting paramagnetic bis-radical $\mathbf{4}^{2(\bullet+)}$. These differences are related to the presence or absence of H-bonds, which govern the relative flexibility or rigidity of the calixarene skeleton. The H-bond free *per*(O-alkylated) calixarene $\mathbf{7}^{4+}$ is flexible enough to allow an effective orbital overlap between the SOMOs of both electrogenerated radical cations. The rigidity of $\mathbf{4}^{4+}$, imposed by the presence of two H-bonds involving adjacent hydroxyl and propoxyl groups (O−H···O−Pr), conversely prevents the calixarene scaffold from adopting a conformation that enables the formation of an intramolecular π-dimer (open bis-radical in Figure 3). This

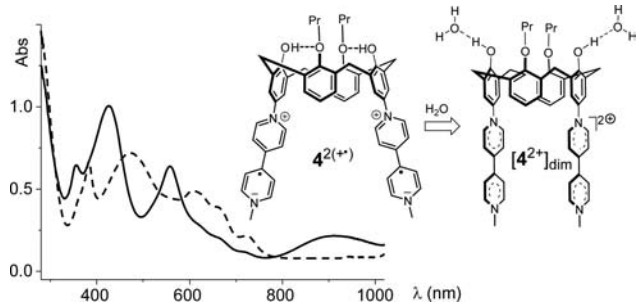

Figure 3. UV/vis spectra (l = 1 cm) of aqueous solutions of $\mathbf{4}^{4+}$ (solid line) and $\mathbf{10}^{2+}$ (dotted line (0.05 mM/$\mathbf{BP}^{2+}$) recorded after reduction with TDAE.

impediment to the π-dimerization of $\mathbf{4}^{4+}$ prompted us to investigate whether a chemical impulse, namely an H-bond competitor, could be used to trigger the formation of the π-dimer $[\mathbf{4}^{2+}]_{dim}$ from the conformationally blocked H-bonded bis-radical $\mathbf{4}^{2(\bullet+)}$.

Reduction experiments were carried out using a chemical reductant in aqueous solution; the presence of water should not only affect the intramolecular H-bonds at the lower rim but also favor the association of the bipyridinium cation radicals at the wider rim due to hydrophobic effects. Formation of $[\mathbf{4}^{2+}]_{dim}$ was achieved from 0.025 mM (0.05 mM per viologen subunit) aqueous solutions of $\mathbf{4}^{4+}$ using tetrakis(dimethylamino)ethylene (TDAE) as the reductant. Unambiguous spectroscopic evidence supporting the formation of the intramolecular dimer $[\mathbf{4}^{2+}]_{dim}$ in water is given by the NIR absorption band centered at 910 nm (Figure 3) which is not observed in the spectrum of the one-electron reduced reference compound $\mathbf{10}^{+\bullet}$. The formation of $[\mathbf{4}^{2+}]_{dim}$ under these conditions results from a combination of two factors: (i) a greater stabilization of the π-dimers of viologen radicals due to hydrophobic effects; (ii) the weakening of the H-bonds involving the phenol moieties. The importance of the hydrophobic contribution is revealed by the fact that DMF, which is a much stronger H-bond acceptor than water, does not promote the intramolecular π-dimerization. It should also be noted that we were unable to disrupt the H-bonding network using various bases. Use of water thus modifies the subtle balance of stabilization energies arising from H-bonding at the lower rim and π-dimerization at the upper rim and favors the formation of $[\mathbf{4}^{2+}]_{dim}$.

Computational studies were carried out on three different viologen-free models to gain insight into the role of the hydroxyl moieties on the π-dimerization of $\mathbf{4}^{4+}$. Previous studies carried out on calixarenes have established that H-bonding might determine the conformation and the rigidity of the calixarene skeleton.[7b,8] The model structures investigated herein display either four hydroxyl substituents ($\mathbf{12}(OH)_4$), two hydroxyl and two propoxyl substituents ($\mathbf{12}(OH)_2(OPr)_2$), or four propoxyl substituents ($\mathbf{12}(OPr)_4$) (Figure 4 and Figure ESI 25).

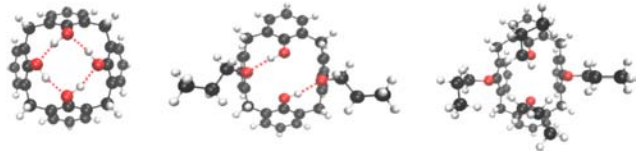

Figure 4. Structures of $\mathbf{12}(OH)_4$ (left), $\mathbf{12}(OH)_2(OPr)_2$ (middle), and $\mathbf{12}(OPr)_4$ (right) optimized at the B3LYP/6-31g(d,p) level.

As seen in the top-views depicted in Figure 4, the conformations of $\mathbf{12}(OH)_4$ and $\mathbf{12}(OH)_2(OPr)_2$ are imposed by the number and the length of the H-bonds involving the four O-atoms. The conformations of both species can be compared using the distances measured at the upper rim between the two pairs of opposite C-atoms located in the para position to the oxygens. In both cases, the distances are too large (8.57 Å for $\mathbf{12}(OH)_4$; 9.58 and 6.73 Å for $\mathbf{12}(OH)_2(OPr)_2$) to allow the existence of interactions between two viologen radicals that would be introduced at the upper rim of the calixarene. In the *per* alkylated compound $\mathbf{12}(OPr)_4$, the absence of H-bonds at the lower rim confers a greater flexibility to the molecule. One consequence of this greater freedom is that the minimized conformation of $\mathbf{12}(OPr)_4$ exhibits one very long (9.97 Å) and most importantly one very short (4.72 Å) interaryl distance. The latter is more favorable to the formation of intramolecular π-dimer species at the upper rim. An estimation of the energy difference between $\mathbf{12}(OH)_2(OPr)_2$ and $\mathbf{12}(OPr)_4$ gives a rough idea of the contribution of the H-bonds energy and thus of the energy cost to be paid to break them. A constrained geometry optimization of $\mathbf{7}^{4+}$ and $\mathbf{4}^{4+}$ was thus carried out using the data calculated for $\mathbf{12}(OPr)_4$ and $\mathbf{12}(OH)_2(OPr)_2$, respectively. The energy difference calculated between $\mathbf{7}^{4+}$ and $\mathbf{4}^{4+}$, kept in the frozen conformations of their model compounds, was $E(\mathbf{7}^{4+}) - E(\mathbf{4}^{4+})$ = +15.8 kcal mol^{-1}. This value suggests that the gain in energy resulting from the interaction between the reduced viologens would have to exceed *ca.* 16 kcal mol^{-1} to counterbalance the stabilization energy of the H-bonds. The structures of $\mathbf{7}^{4+}$ in its ground and reduced states were also optimized. Minimization of the doubly reduced species generates $[\mathbf{7}^{2+}]_{dim}$ (Figure 5), wherein both bipyridinium cation radicals are in a sandwich-like conformation with inter-ring distances ranging from 3.3 to 3.8 Å. The calixarene skeleton appears slightly distorted compared to that calculated for the viologen-free model $\mathbf{12}(OPr)_4$ with a distance of *ca.* 4.2 Å measured between the two carbons connecting the calixarene to the viologens. In contrast, the minimized structure of $\mathbf{4}^{2(+\bullet)}$ was an "open" conformation that prohibits interactions between both viologen cation radicals.

DOI: 10.1021/acs.orglett.5b01982
Org. Lett. 2015, 17, 4058−4061

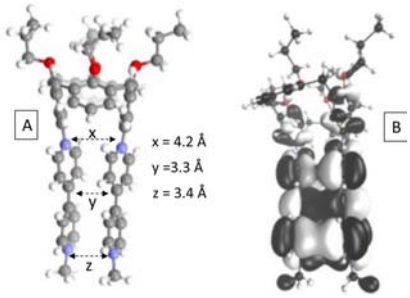

Figure 5. Schematic representation of the interaction between two viologen cation radicals in $[7^{2+}]_{dim}$. A: Optimized structure of $[7^{2+}]_{dim}$ at the BLYPD/DZVP level and B: HOMO of $[7^{2+}]_{dim}$.

The viologens in the oxidized structure $\mathbf{4}^{4+}$ are structurally similar to those in 7^{4+} (tilt angle of 35° and C−C distance of 1.48 Å). In agreement with the experimental studies carried out in water, the inclusion of two water molecules leads to the cleavage of both H-bonds involving the phenol subunits and to the concomitant formation of the dimerized species $[\mathbf{4}^{2+}\cdot(H_2O)_2]_{dim}$.

In conclusion, Zincke-like reactions have been implemented to synthesize a series of viologen-calixarene conjugates featuring two viologen units introduced without linkers at the upper rim of a calixarene skeleton. The title compounds differ by their substitution pattern of the four OH functions at the lower rim. Our results demonstrate that π-dimerization can be enhanced and controlled by the use of a semirigid calixarene platform. Formation of an intramolecular π-dimer in the two-electron-reduced state is especially supported by the extension of the electrochemical stability domain of the reduced species, the loss of ESR signature, and the appearance of a characteristic NIR absorption band. The ability of the phenol-containing calixarene $\mathbf{4}^{4+}$ to dimerize depends on a subtle balance of weak interactions associated with (*i*) H-bond formation at the lower rim and (*ii*) orbital overlap between π-radicals on the upper rim. In DMF, the stabilization energy associated with H-bonding is predominant and π-dimerization is precluded. In aqueous media, π-dimerization, mainly stabilized by hydrophobic effects, governs the conformation of the molecule. This work not only provides experimental evidence for the weak nature of the forces involved in long-bonded π-dimers but also gives access to a dually responsive molecular object controlled by a subtle combination of electrochemical and chemical stimuli.

■ ASSOCIATED CONTENT

Supporting Information

The Supporting Information is available free of charge on the ACS Publications website at DOI: 10.1021/acs.orglett.5b01982.

Experimental procedures, spectral and computational data (PDF)

■ AUTHOR INFORMATION

Corresponding Authors

*E-mail: christophe.bucher@ens-lyon.fr.
*E-mail: eric.saint-aman@ujf-grenoble.fr.

Notes

The authors declare no competing financial interest.

■ ACKNOWLEDGMENTS

This work was supported by the "Agence National de la Recherche" (ANR-12-BS07-0014-01), by the "Institut de Chimie de Lyon" (NitroFer project), by the Labex Arcane (ANR-11-LABX-0003-01), and by IDRIS (project i2014086670).

■ REFERENCES

(1) (a) Kahlfuss, C.; Saint-Aman, E.; Bucher, C. Redox-controlled intramolecular motions triggered by π-dimerization and pimerization processes. In *Organic Redox Systems: Synthesis, Properties, and Applications*; Nishinaga, T., Ed.; John Wiley and Sons: New-York, 2016; Vol. in press. (b) Zhang, D.-W.; Tian, J.; Chen, L.; Zhang, L.; Li, Z.-T. *Chem. - Asian J.* **2015**, *10*, 56.

(2) (a) Spruell, J. M. *Pure Appl. Chem.* **2010**, *82*, 2281. (b) Nishinaga, T.; Komatsu, K. *Org. Biomol. Chem.* **2005**, *3*, 561. (c) Le Poul, N.; Colasson, B. *ChemElectroChem* **2015**, *2*, 475. (d) Fahrenbach, A. C.; Bruns, C. J.; Li, H.; Trabolsi, A.; Coskun, A.; Stoddart, J. F. *Acc. Chem. Res.* **2014**, *47*, 482. (e) Fahrenbach, A. C.; Warren, S. C.; Incorvati, J. T.; Avestro, A.-J.; Barnes, J. C.; Stoddart, J. F.; Grzybowski, B. A. *Adv. Mater.* **2013**, *25*, 331.

(3) (a) Iordache, A.; Kannappan, R.; Métay, E.; Duclos, M.-C.; Pellet-Rostaing, S.; Lemaire, M.; Milet, A.; Saint-Aman, E.; Bucher, C. *Org. Biomol. Chem.* **2013**, *11*, 4383. (b) Iordache, A.; Melfi, P.; Bucher, C.; Buda, M.; Moutet, J.-C.; Sessler, J. L. *Org. Lett.* **2008**, *10*, 425. (c) Iordache, A.; Oltean, M.; Milet, A.; Thomas, F.; Saint-Aman, E.; Bucher, C. *J. Am. Chem. Soc.* **2012**, *134*, 2653. (d) Iordache, A.; Retegan, M.; Thomas, F.; Royal, G.; Saint-Aman, E.; Bucher, C. *Chem. - Eur. J.* **2012**, *18*, 7648. (e) Kahlfuss, C.; Métay, E.; Duclos, M.-C.; Lemaire, M.; Milet, A.; Saint-Aman, E.; Bucher, C. *Chem. - Eur. J.* **2015**, *21*, 2090. (f) Kahlfuss, C.; Métay, E.; Duclos, M.-C.; Lemaire, M.; Oltean, M.; Milet, A.; Saint-Aman, E.; Bucher, C. *C. R. Chim.* **2014**, *17*, 505.

(4) (a) Song, C.; Swager, T. M. *Org. Lett.* **2008**, *10*, 3575. (b) Pognon, G.; Boudon, C.; Schenk, K. J.; Bonin, M.; Bach, B.; Weiss, J. *J. Am. Chem. Soc.* **2006**, *128*, 3488. (c) Lyskawa, J.; Salle, M.; Balandier, J.-Y.; Le Derf, F.; Levillain, E.; Allain, M.; Viel, P.; Palacin, S. *Chem. Commun.* **2006**, 2233. (d) Lyskawa, J.; Canevet, D.; Allain, M.; Sallé, M. *Tetrahedron Lett.* **2010**, *51*, 5868. (e) Düker, M. H.; Gómez, R.; Vande Velde, C. M. L. V.; Azov, V. A. *Tetrahedron Lett.* **2011**, *52*, 2881. (f) Düker, M. H.; Schäfer, H.; Zeller, M.; Azov, V. A. *J. Org. Chem.* **2013**, *78*, 4905.

(5) (a) Verboom, W.; Datta, S.; Asfari, Z.; Harkema, S.; Reinhoudt, D. N. *J. Org. Chem.* **1992**, *57*, 5394. (b) Iwamoto, K.; Araki, K.; Shinkai, S. *Tetrahedron* **1991**, *47*, 4325. (c) Kelderman, E.; Verboom, W.; Engbersen, J. F. J.; Reinhoudt, D. N.; Heesink, G. J. T.; van Hulst, N. F.; Derhaeg, L.; Persoons, A. *Angew. Chem., Int. Ed. Engl.* **1992**, *31*, 1075. (d) van Wageningen, A. M. A.; Snip, E.; Verboom, W.; Reinhoudt, D. N.; Boerrigter, H. *Liebigs Annalen* **1997**, *1997*, 2235. (e) Liang, Z.; Liu, Z.; Jiang, L.; Gao, Y. *Tetrahedron Lett.* **2007**, *48*, 1629.

(6) (a) Coe, B. J.; Harries, J. L.; Helliwell, M.; Jones, L. A.; Asselberghs, I.; Clays, K.; Brunschwig, B. S.; Harris, J. A.; Garin, J.; Orduna, J. *J. Am. Chem. Soc.* **2006**, *128*, 12192. (b) Constantin, V.-A.; Cao, L.; Sadaf, S.; Walder, L. *Phys. Status Solidi B* **2012**, *249*, 2395.

(7) (a) Kim, S. K.; Lynch, V. M.; Hay, B. P.; Kim, J. S.; Sessler, J. L. *Chem. Sci.* **2015**, *6*, 1404. (b) Pognon, G.; Wytko, J. A.; Harvey, P. D.; Weiss, J. *Chem. - Eur. J.* **2009**, *15*, 524.

(8) (a) Aleman, C.; Zanuy, D.; Casanovas, J. *J. Org. Chem.* **2006**, *71*, 6952. (b) Zanuy, D.; Casanovas, J.; Aleman, C. *J. Phys. Chem. B* **2006**, *110*, 9876. (c) Casanovas, J.; Zanuy, D.; Aleman, C. *Angew. Chem., Int. Ed.* **2006**, *45*, 1103.

DOI: 10.1021/acs.orglett.5b01982
Org. Lett. 2015, 17, 4058−4061